Detection of pulmonary thrombembolism and postmortem clotting on postmortem magnetic resonance imaging

Flach, P M ; Franckenberg, Sabine ; Gascho, Dominic ; Ampanozi, Garyfalia ; Thali, Michael J ; Fliss, B

DOI: https://doi.org/10.1016/j.fri.2023.200574

Forensic Imaging 36 (2024) 200574

Contents lists available at ScienceDirect

Forensic Imaging

journal homepage: www.sciencedirect.com/journal/forensic-imaging

Detection of pulmonary thrombembolism and postmortem clotting on postmortem magnetic resonance imaging

P.M. Flach [a,1], S. Franckenberg [b], D. Gascho [a], G. Ampanozi [a], M.J. Thali [a], B. Fliss [c,*]

[a] Institute of Forensic Medicine, University of Zurich, Winterthurerstrasse 190/52, Zurich 8057, Switzerland
[b] Institute of Diagnostic and Interventional Radiology, University Hospital Zurich, Raemistrasse 100, Zurich 8091, Switzerland
[c] Institute of Forenisc Medicine, University Medical Center of the Johannes Gutenberg-University Mainz, Am Pulverturm 3, Mainz 55131, Germany

ARTICLE INFO

Keywords:
Postmortem imaging
Postmortem MRI
Pulmonary thrombembolism
Postmortem clotting

ABSTRACT

The purpose of this study was to develop a feasible imaging protocol superior to postmortem computed tomography (PMCT) and to establish diagnostic parameters for diagnosing pulmonary thromboembolism (PE) on postmortem magnetic resonance imaging (PMMR).

The study collective of 113 subjects was prospectively investigated by PMMR for the presence of PE and / or postmortem clotting (cruor). PE was detected in 20 cases; the remaining 93 cases were investigated for the morphology of cruor. Age grading was performed by PMMR, autopsy and histology. The postmortem sedimentation effect was used for the applied imaging protocol on PMMR (supine and prone position). Visual distension of the pulmonary arteries in PE was seen in all cases, but not in the controls. Re-positioning of the corpse from supine in prone position proved to be beneficial in 90 %. Postmortem motion artifacts are firstly described in 20.4 %. Hyperacute PE (grade 1) presented with a homogenous and hypointense signal on T2w images, acute PE (grade 2) with slightly heterogeneous, but still homogenous hypointense signal, subacute PE (grade 3) was with heterogeneous and slightly hyperintense signal and chronic PE (grade 4) with predominately homogenous with scarce portions of heterogeneous but hyperintense signal. PMMR allowed for the detection of PE and for *in situ* depiction of combined age grading.

Introduction

Postmortem imaging, one of the most recent advancements in forensic medicine, has swiftly evolved into a standard procedure for forensic investigations in many countries [1–5]. Currently, dedicated postmortem computed tomography scanners are installed in various morgues, forensic institutes, or clinical settings, allowing forensic pathologists to use them. These scanners are used in daily routines either as triage tool, as primary diagnostic method or, most commonly, as supplement to forensic autopsies [6–8].

Despite the increasing embrace of new technological advancements by forensic institutes, postmortem magnetic resonance imaging (PMMR) has not yet become a routine modality in the majority of centers. Instead, it is primarily used for research in affiliated institutes [5]. PMMR, however, is an adjunct modality to PMCT excelling in depicting soft tissue and parenchymal pathologies [5]. Major publications of PMMR often focus on imaging fetuses, newborns, infants or cardiac pathologies [9–17]. Additionally, research in PMMR research extends to imaging of the head and neck region, as well as whole body imaging [5, 18–23]. The reluctance towards PMMR as a routine tool is most probable related to the necessity of trained personnel due to its complexity, the costs associated with equipment acquisition and maintenance, and notably, the time required for image acquisition compared to than PMCT.

The European guidelines for the diagnosis and management of pulmonary thromboembolism (PE) report annual incidence rates of venous thrombosis and PE of approximately 0.5 to 1.0 per 1000 inhabitants or even accounts for up to 15 % of diagnosis finally identified during conventional autopsy [24–27]. PE is a common cause of death for hospitalized patients indicated by elevated risk factors accompanying hospitalization or increased presence of predisposing pathologies [28]. Nevertheless, PE is also a common natural cause of death in the forensic case collective as those deaths usually occur suddenly and unexpected [29]. Therefore, imaging should yield for a reliable way to diagnose PE

* Corresponding author.
E-mail address: fliss@uni-mainz.de (B. Fliss).
[1] Passed away in March 2021

https://doi.org/10.1016/j.fri.2023.200574

Available online 21 December 2023

despite postmortem changes such as postmortem clotting – especially if imaging is the sole diagnostic tool used.

A typical postmortem change due to a lack of circulation is sedimentation, leading to a position-dependent layered appearance of corpuscular blood particles. This includes erythrocytes settling at the base, exhibiting a homogenous hypointense signal, while the hyperintense plasma settles atop the descended erythrocytes on T2w images [3–5]. This phenomenon is gravidity dependent and was used as diagnostic asset for the underlying study [5]. The sedimentation effect may be affected by the presence of postmortem blood clots (cruor), which should not be confused with antemortem PE. These clots typically exhibit a position-dependent nature and are therefore also gravity-dependent within the pulmonary trunk, arteries, heart chambers, and other major vessels [5,30]. Occasionally, the entire pulmonary trunk and bifurcation is filled with cruor and may leave no or little space for the typical appearance of layered erythrocytes and plasma within the pulmonary arteries.

The occurrence of postmortem clotting may mimic PE and poses the major obstacle of a reliable diagnosis of PE on postmortem imaging [31]. The signal intensity of postmortem clots is greatly influenced by the type of cruor either red currant jelly or chicken fat clot or combined, that are present [5]. Red currant jelly cruor occurs more rapidly than the slowly sedimenting chicken fat clot. In accordance to their name they resemble in form and texture either red currant jelly or chicken fat. Examined histologically the red currant jelly clot contains unorganized fibrin, erythrocytes and leucocytes. The chicken fat clot on the other hand contains predominantly of leucocytes and fibrin (for examples see Figs. 5 and 6). The appearance of PE seems to differ by age of the vitally embolized clot leaving multiple hurdles in properly differentiating PE from cruor in a postmortem setting.

The purpose of this study was to develop a feasible imaging protocol superior to PMCT and to establish diagnostic parameters for diagnosing pulmonary thromboembolism on PMMR.

Materials and methods

Postmortem imaging

This prospective study was performed over a 35 months period (February 2013 to March 2016). Each corpse received a full-body PMCT scan using a dual-source 128-slice scanner (SOMATOM Flash Definition, Siemens Medical Solutions, Forchheim, Germany) with standard scan parameters at a 120 kVp tube voltage with automated dose modulation, with parameters according to the literature [32]. Reconstructions were made in a soft tissue window with a soft kernel and bone window with a hard kernel in an adjusted field of view. The study subjects were consecutively included if cardiac failure was a probable cause of death pronounced at the scene after an external examination. Exclusion criteria were other probable causes of death based on history, circumstances and PMCT imaging results as pre-selection tool as well as decomposition.

PMMR imaging was performed using a 3.0-Tesla MR (Achieva TX, Philips, Best, the Netherlands) after each case that was delivered to the morgue had received a whole-body PMCT. Each evaluated case underwent a standard heart protocol using an 8-element phased-array coil. The protocol was either based on a standardized heart protocol including supine imaging of PE, or it was performed as sole PE protocol. In some cases, both protocols were combined.

The standard cardiac protocol consisted of T2w sequences with a 4-chamber and short axis view as well as proton density, hemo-sensitive, T2w fat-saturated (FS) and T1w sequences in short axis views for diagnosis of potential myocardial pathology [5]. This protocol also included 3 additional sequences - all in supine position - such as axial T2w spectral attenuated inversion recovery (SPAIR) (TR 5401.6, TE 60.0) and T1w (TR 624.7, TE 6.4) sequences in 3 mm and T2w (TR 4178.1, TE 100.0) in 1.5 mm aligned to the pulmonary arteries [5].

The dedicated PE protocol included the above mentioned 3 sequences in supine as well as in prone position, meaning that the corpse was turned after supine scan in prone position for reapplying the protocol with identical parameters. When both protocols were applied the entire cardiac protocol was executed as well as the additional sequences in prone position.

The exact scanning parameters as well as the duration are listed in Table 1.

PMMR image review

For radiological assessment, a multi-modality workstation was used (Syngo via, Version VB10A, Siemens, Medical Solutions, Erlangen, Germany). A forensic experienced board-certified radiologist performed radiological analysis and reporting.

The T2w SPAIR sequence, with manual signal alteration and magnification in both supine and prone positions (if both were performed), was primarily used for assessment. The thin-sliced T2w FS sequence was only occasionally utilized to verify the diagnosis and exclude partial volume effects or other biases. Signal windowing of T2w images was set with a width of 380 and a center of 155 for evaluation

The PMMR images were assessed for the presence of PE and / or cruor (postmortem clotting), visual distension of the pulmonary arteries, the relocation of intraluminal clots (PE and cruor) and subsequently adhesion to the vascular wall after reposition. The assessment was limited to the pulmonary trunk and both main pulmonary arteries. Segmental or subsegmental evaluation was not performed on PMMR. Morphology and signal intensity observed on PMMR was correlated to the age grading based on histology,similar to the process used in hematoma imaging on clinical magnetic resonance imaging [30,33]. Grade 1 related to hyperacute PE, grade 2 to acute PE, grade 3 to subacute PE and grade 4 to chronic PE. The responsible justice department approved postmortem imaging examinations and mandated forensic autopsy. The study was conducted according to the guidelines of the Declaration of Helsinki and approved by the Ethics Committee Zürich (KEK-ZH No: 2015–0686).

Study collective

A total of 113 subjects were evaluated for pulmonary thromboembolism (PE) by PMMR. The study population consisted of 67 males and 46 females with a range of age from 17 to 89 years (mean 55.8 years, median 53 years). According to the inclusion criteria all cases in which a cardiac arrest was the supposed cause of death at the scene were included. Throughout the investigation, this supposed cause of death was confirmed in 98 subjects. In 15 cases, the cause of death was changed (central regulatory arrest n: 10; drowning n: 5).

Manner of death was in the majority of cases natural death (n: 88), followed by accident (n: 18). Aside from that, there was one case of suicide and one case with complications in the course of a surgical intervention. There were 5 remaining cases that remained unresolved and it could not be definitely determinded whether it was a suicide or an accident (n: 4) or whether it was an accident or a natural death (n: 1).

The overall postmortem interval from time of death to PMMR scan ranged from 2 to 168 h (mean 31.6 hours, median 24 h). The overall postmortem interval from time of death to autopsy ranged from 4 to 190 h (mean 41.6 h, median 34.5 h).

Autopsy

Conventional autopsy included dissection of the three body cavities (skull, thorax and abdomen) as well as preparation of the larynx and was performed in each evaluated case. Autopsy was performed by a board-certified forensic pathologist and a resident.

For each case with PE the written description (hyperacute, acute, subacute, chronic) of the official report and photographs were assessed

Table 1
Scanning parameters for PMMR. TR = repetition time, TE = echo time, SL = slice thickness, NSA = number of averages, TSE = turbo spin echo, f = factor, (s) = shortest, SPIR = spectral presaturation inversion recovery, (r) = range, FFE = fast field echo, (ip) = in-phase, PD = proton density, SPAIR = spectral attenuated inversion recovery, BoPT = bifurcation of pulmonary trunk. Note: Due to the "shortest" settings the corresponding TR/TE can change and thus shorten the time required for the sequence.

	Orientation	Weighting	Acquisition	TR [ms]	TE [ms]	Flip angle	Slices	SL [mm]	Overlap [mm]	Matrix	NSA	Time [mm: ss]
Cardiac	4-chamber	T2	TSE (f:17)	3030(s)	100	90	30	3	0.3	884x663	4	10:43
Cardiac	short axis	T2	TSE (f:17)	4040(s)	100	90	40	3	0.3	884x663	3	10:40
Cardiac	short axis	T2 SPIR	TSE (f:11)	2010(s)	60	90	30	3	0.3	776x583	4	09:31
Cardiac	short axis	T1	TSE (f:5)	674(r)	10(s)	90	30	3	0.3	1032x775	4	10:39
Cardiac (optional)	short axis	T2*	FFE	3250(s)	16(ip)	18	30	3	0.3	444x443	2	10:19
Cardiac (optional)	short axis	PD	TSE (f:12)	1800	25	90	30	3	0.3	888x648	4	09:43
PE	transversal	T2 SPAIR	TSE (f:18)	5402(s)	60	90	55	3	1	412x368	3	13:22
PE	transversal	T1	TSE (f:5)	625(r)	6.4(s)	90	55	3	1	472x430	2	12:09
PE	BoPT	T2	TSE (f:24)	4178(s)	100	90	35	1.5	0.15	660x576	4	13:56

Table 2
Overview of the grading of PE in all cases regarding histology, autopsy and PMMR. (Legend: * histology of segmental pulmonary artery, L left side, paracentral pulmonary artery, R right side, paracentral pulmonary artery, n.a. not assessable, 0 no histology taken, + positive, ++ predominant positive stage, - negative, (+) slight characteristics).

	Histology								Autopsy					PMMR							
Stage	1		2		3		4		1	2	3	4	5	1		2		3		4	
Case No.	L	R	L	R	L	R	L	R	no specific description of side affiliation					L	R	L	R	L	R	L	R
1	-	-	-	-	-	-	+	-	-	-	-	+ (L)	-	-	-	-	-	-	-	+	-
2	n.a.	n.a.	n.a.	n.a.	n.a.	n.a.	n.a.	n.a.	-	-	-	+	+	-	-	-	-	-	-	+	+
3	+	+	+	+	-	-	-	-	-	+	+	-	-	-	-	+	+	-	-	-	-
4	+	+	-	-	-	-	-	-	+	+	+	-	-	+	+	(+)	+	-	-	-	-
5	0	0	0	0	0	0	0	0	+	-	-	-	-	+	+	+	+	+	+	-	-
6	+	+	+	+	+	+	-	-	+	-	-	-	-	+	+	+	(+)	+	+	-	-
7	+	+	-	-	-	-	-	-	-	+	-	-	-	+	+	+	+	+	+	-	-
8	++	-	+	+	-	-	-	-	-	+	-	-	-	+	+	+	+	-	-	-	-
9	-	+	+	-	-	-	-	-	+	-	-	-	-	+	+	+	+	-	-	-	-
10	0	0	0	0	0	0	0	0	+	-	-	-	-	-	+	+	+	+	+	(+)	-
11	+	+	-	-	+	+	-	-	+	+	-	-	-	+	+	+	+	+	-	-	-
12	+	+	-	-	-	-	-	-	+	-	+	-	-	+	+	+	+	+	+	-	+
13	-	+	-	-	-	-	+	-	+	+	-	+	-	-	-	+	+	-	-	+	-
14	0	0	0	0	0	0	0	0	-	+	-	+	-	+	-	+	+	-	-	+	-
15	+	+	-	-	-	-	-	-	+	+	-	-	-	+	+	+	-	-	-	-	-
16	+	+	-	-	-	-	-	-	+	-	-	-	-	+	+	-	-	-	-	-	-
17	-	-	+	+	-	-	-	-	+	-	-	-	-	-	-	+	+	+	+	-	-
18	+	+	-	-	-	-	-	-	+	+	+ (R)	-	-	+	+	+	+	-	-	-	-
19	+	+	-	-	+	+	-	-	+	-	-	-	-	+	+	+	+	+	+	+	-
20	-	-	+	+	-	-	-	-	+	-	-	-	-	+	+	+	+	-	+	-	-

and compared to the findings of PMMR and histology.

Differential diagnosis between PE and cruor was based on established literature [30]. A red thrombus of PE presented macroscopicallywith a smooth surface, a somewhat elastic consistence, was, wall-adherent and dry-damp with lividity in its progression [30]. The white thrombus of PE was determined when dry, partially brittle and wall-adherent, with finely striated surface and with partially gray-red portions and its border unrelated to the position of the body [30].

Macroscopically the cruor may appear as a “red currant jelly clot” presenting with a more reflective surface, dark red (partially livid) color, smooth with a glistening surface and not attached to the intimal [5,30, 34]. These darker bands of cruor are usually composed of layered erythrocytes “red-cell rich” coagulum with scattered white cells. The other portion of the cruor called “chicken fat clot” consists primarily of fibrin and is composed of platelets mixed with fibrin, leukocytes and plasma “red-cell poor” and appears therefore greyish, yellow to white also with a smooth and shiny surface [5,34]. If no movement of the body occurred a clear and often horizontal border presents between the portions of the cruor. The chicken fat clot is described as forming slower than the red currant jelly clot [34].

Histology

Histology was performed in 17 of the 20 cases with PE. Histological assessment was not possible in one case due to flawed storage of the specimen. In total, histology in 16 cases was evaluated. Histology was taken from both sides of the clots within the right and left pulmonary arteries, if present on both sides. Staining included hematoxylin and eosin (HE) stain and Elastica van Gieson stain (EvG) of pulmonary thromboembolism. Fixation in 10 % formaldehyde was done prior to slicing specimen.

The histology was graded according to the chronology of histologically microscopically detecTable organization of a thrombus or thromboembolism [30]. Grade 1 (day 2: day 1 to 3) was defined as no reaction between vascular endothelium and thrombus and present continuity of basal membrane and endothelium, referred to as hyperacute grade in this study [30]. Grade 2 (day 5: day 3 to 8) was related early “endothelization” of the thrombus surface with centrally originating “hyalinization” of the thrombotic material, referred to as acute grade in this study [30]. Grade 3 (day 10: day 4 to 20) correlated to migrated fibroblasts, fibrocytes and mesenchymal cells from the macroscopic wall-adherent portion and hemosiderin pigment-laden macrophages and branched endothelium wrapped capillaries, here referred to as subacute stage [30]. Grade 4 (week 3-4: day 8 to 2 months) related to pronounced capillarization, collagen and fibroplasia and leukozytic debris within hyalinized areas [30]. Grade 5 and 6 was not seen in any specimen and therefore not listed here.

Histology of cruor was only taken if PE was not macroscopically

determinable with the same staining as PE specimen. Histology was assessed by a board-certified forensic pathologist experienced in forensic imaging.

Results

In total, the majority of cases (n: 62) underwent the dedicated PE protocol (imaging in supine and prone position). The Cardiac protocol including supine PE imaging was performed in 16 cases and additional 35 cases underwent both complete protocols (PE protocol and Cardiac protocol).

From the 113 cases, 20 cases were confirmed as PE in autopsy as well as by PMMR (7 males, 13 females) with a range of age from 36 to 87 years (mean 62.1 years, median 59 years), 18 with natural death and 2 with accident as manner of death. The postmortem interval from time of death to PMMR ranged in this collective from 2 to 58 h (mean 22.5 h, median 14 h). The postmortem interval from time of death to autopsy ranged from 4 to 67 h (mean 29.3 h, median 24.5 h). The used imaging protocol was predominantly (n: 16) the dedicated PE protocol (supine and prone position), three cases underwent additional cardiac protocol and only one case received the cardiac protocol (including supine PE imaging).

The remaining 93 cases (60 males, 33 females) did not exhibit PE and were evaluated for the morphology of cruor. The postmortem clotting (cruor) case collective ranged from 17 to 89 years (mean 54.4 years, median 53 years). The most common cause of death was cardiac arrest (n: 78), central regulatory failure was diagnosed in 10 cases and asphyxia in drowning in 5 subjects. The predominant manner of death was natural death (n: 71), followed by accident (n: 15), complication in the course of surgical intervention (n: 1) and one case as suicide. The remaining 5 subjects were not conclusively defined and presented with either accident vs. suicide (n: 4) or accident vs. natural death (n: 1). A dedicated PE protocol in supine and prone position in 46 cases and almost equally often PE and cardiac protocol was used (n: 32). Only 15 cases underwent sole cardiac imaging (including supine PE protocol).

PMMR

PE vs. postmortem clotting

PE was present in 20 cases (17.7 %) of all 113 investigated cases, the remaining 93 cases showed only cruor. PE was dominant in the female case collective (female 65 %, male 35 %). The collective without PE presented the opposite way around with more males (females 35.5 %, males 64.5 %).

The distribution of PE was centrally located in 9 cases (45 %), unilaterally accentuated but central in 2 cases (10 %), para-centrally (in both pulmonary arteries, but not crossing the trunk) in 6 cases (30 %) and unilateral in one side of the pulmonary arteries in 3 cases (15 %).

Vascular distension on PMMR

All cases with PE exhibited a visual distension of the pulmonary arteries at the location where PE was present with slight buckling of the vascular wall (Fig. 1). All cases with cruor did not exhibit this sign.

Wall-adherent position on PMMR

In addition, 18 cases (90 %) did not exhibit any relocation of the PE after re-positioning from supine into prone position and where therefore determined as wall-adherent (Fig. 2). Only 2 cases (10 %) with hyperacute PE showed scarce partial movement after re-positioning but remained still wall-adherent. All cases with cruor showed movement of the intraluminal clot and a re-distribution of plasma and sediment (if present) according to gravidity between the clot and the vascular wall

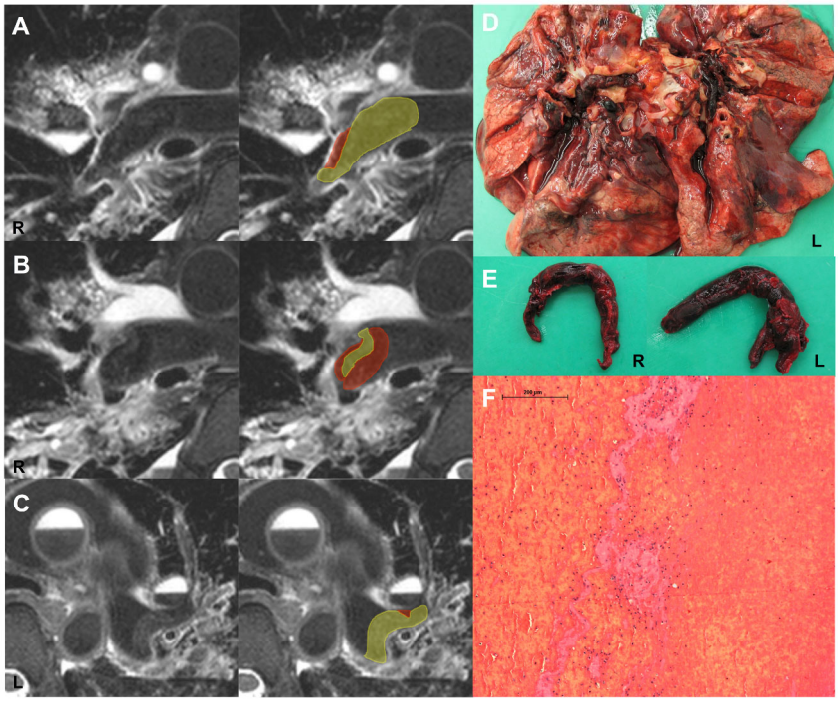

Fig. 1. This Figure is case 4 (Table 2). A and B show PMMR with a detailed view on the right main pulmonary artery. C shows a detailed view on the left main pulmonary artery. The left image column displays the detailed view on the right pulmonary artery and the right column displays the same image with highlighted PE. This case exhibits grade 1 and 2 according to hyperacute (colored in red) to acute (colored in yellow) PE on PMMR. The hyperacute portion of the thrombus presents with a homogenous and hypointense (a little darker than the surrounding sediment) signal on T2w images. The acute portion of the PE is slightly more heterogeneous but vastly homogenous with still hypointense signal on T2w images. D shows the macroscopic view with the PE still lodged within the pulmonary arteries. Image E displays the dislodged thromboembolism of the right and left side. Macroscopic assessment stated grade 1 to 3 (hyperacute to subacute). Histology (magnified view) in HE shows hyperacute red thrombus with homogenous distribution of erythrocytes and without detectable layering according to grade 1 (hyperacute) PE. Note the typical sedimentation effect within the major vessels (ascending aorta, pulmonary trunk and veins in this case, image A-C).

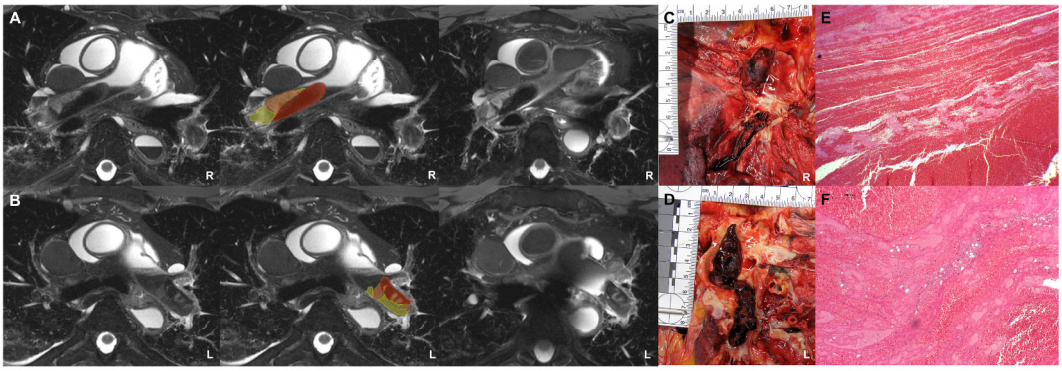

Fig. 2. This Figure relates to case 6 (Table 1). The upper row (A) shows the right main pulmonary and the lower row (B) the left pulmonary artery. The left sided image in each row was obtained in supine position; the image in the middle is same image as on the left with highlighted PE and the right image shows same pulmonary artery in prone position. The sedimentation is not definitive in its full extent. This case shows hyperacute to subacute morphology (hyperacute red, acute, yellow, subacute orange) on both sides on PMMR. The signal varies from homogenous hypointense (grade 1) to heterogeneous and slightly hyperintense signal (grade 3). C shows the macroscopic view of the right main pulmonary artery and D the left main pulmonary artery, both graded hyperacute (grade 1) during autopsy. Histology evaluated grade 1 to 3 (hyperacute to subacute) completely confirming PMMR results. E displays grade 1 and 2 (hyperacute to acute, HE) with early endothelization and centrally originating hyalinization. F shows grade 1 and 3 (hyperacute and subacute, HE) with migrating fibroblast, fibrocytes, mesenchymal cells and macrophages as well as branched endothelium-wrapped capillaries.

allowing for delineation of cruor on the anterior vascular wall in supine and on the posterior vascular wall in prone position, except for cases where the entire pulmonary trunk and main pulmonary arteries where filled with material.

Signal morphology on PMMR

Sediment of erythrocytes presented homogenous and strongly hypointense; and the plasma homogenous and strongly hyperintense on T2w images. Sediment was present as well in PE as in cruor.

Pulmonary thromboembolism

Hyperacute PE (grade 1) presented with a homogenous and hypointense signal on T2w images (Fig. 1). Acute PE (grade 2) showed slightly heterogeneous, but vastly still homogenous and hypointense signal on T2w (Figs. 1, 2). Subacute PE (grade 3) was assessed by a heterogeneous and slightly hyperintense signal and chronic PE (grade 4) was predominately homogenous with scarce portions of heterogeneous but hyperintense signal (Figs. 2–4). In the majority of cases more than only one grade but rather fresh and older portions of PE were seen on PMMR (Table 1). Only 4 cases displayed one isolated grade on PMMR (grade 1 n:1, grade 2 n:1, grade 4 n:2) (Fig. 4). Most cases (n: 16) exhibited a combined morphology (grade 1+2 n:5, grade 1-3 n:5, grade 1-4 n:3, grade 2+4 n:1, grade 1+2+4 n:1, grade 2+3 n:1) (1-3).

Isolated hyperacute PE was evaluated in 5 % (grade 1, n:1). Hyperacute to acute PE (grade 1+2) was detected on PMMR in 35 % (n:7) and combined morphology including hyperacute to subacute was seen in 90 % of the cases (Table 1). Hyperacute to subacute PE (grade 1-3) was seen in 65 % (n: 13). Isolated chronic grade (grade 4) of PE was only detected in 10 % (n:2).

Cruor

The cruor pattern was homogenous hypointense in the red currant jelly clot and was heterogeneous hyperintense in the chicken fat clot (Figs. 5, 6). Mixed forms with scarce discrimination between the portions were also detecTable and are referred to as mixed forms (Fig. 6).

Mixed forms posed the majority of cases (35 %). In the majority of this pattern distinct chicken fat clot was visible in 70 % of the mixed cases, 30 % displayed no delineable chicken fat clot but rather signal

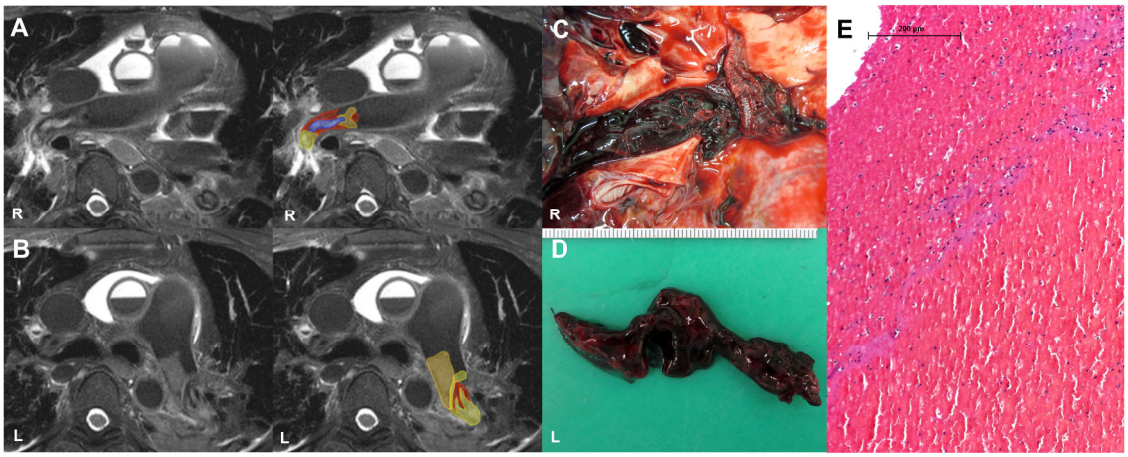

Fig. 3. This Figure relates to case 12 (Table 2). A displays the main right pulmonary artery and B the left main pulmonary artery, on the left detail view of PMMR and on the right PE color highlighted. PMMR analysis detected grade 1 to 4 within the right pulmonary artery and on the left grade 1 to 3. Grade 4 (chronic, colored in blue) shows a predominantly homogenous with scarce portions of heterogeneous but hyperintense signal. Hyperacute is colored in red, acute in yellow and subacute in orange, respectively. C exhibit the gross anatomy during autopsy of the right main pulmonary artery and D the dislodged thrombus of the left side graded as hyperacute and subacute in autopsy (grade 1 and 3). Histology (image E, HE staining) yielded only grade 1 (hyperacute) and probably only represent a portion of the entire thrombus.

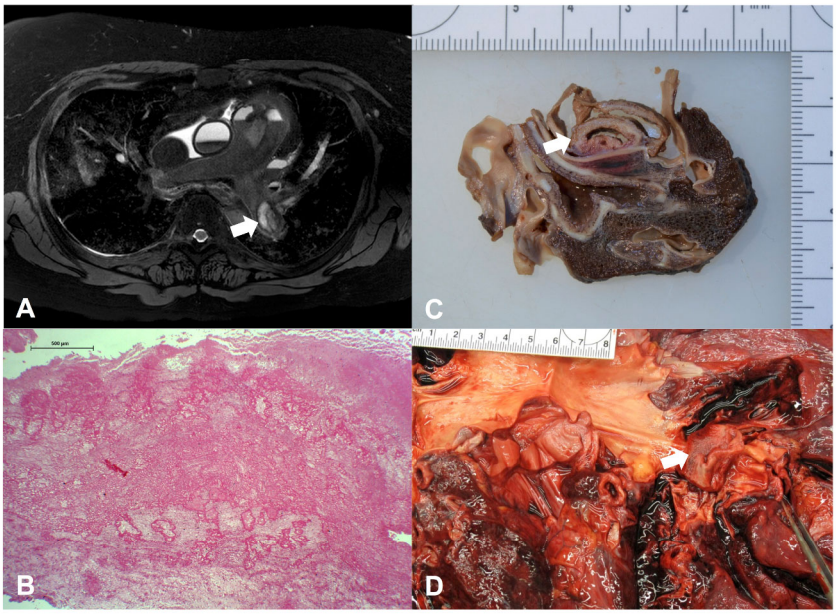

Fig. 4. A shows PMMR T2w sequence with PE in the left main pulmonary artery being assessed as grade 4 only. This case related to case 1 in Table 2. The chronic grade (grade 4) shows a predominately homogenous with scarce portions of heterogeneous but hyperintense signal on T2w (white arrow). Histology (image B, HE) showed according to PMMR analysis a chronic grade with advanced thrombus organization with branched capillary blood vessels and macrophages. C shows the fixed specimen in formaldehyde including PE (white arrow), the pulmonary artery and lung parenchyma. Autopsy did also coincide with the PMMR and histology results of grade 4. D shows the corresponding autopsy specimen with PE (white arrow) in the left pulmonary artery.

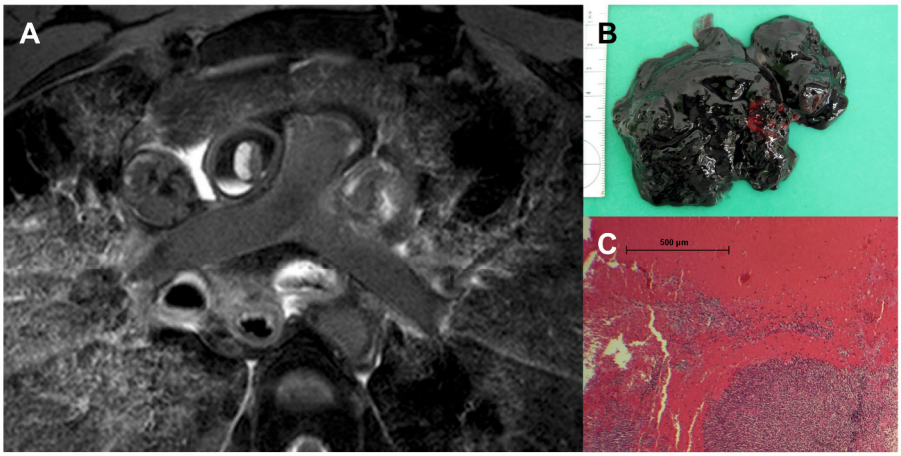

Fig. 5. This Figure shows an entirely filled pulmonary trunk and main pulmonary artery on both sides with a vast red currant jelly clot (cruor) as is was seen in 10.5 % of all cruor cases (A). PMMR is obtained in prone position and a re-positioning of the cruor was not feasible. B shows the dislodged red currant jelly clot during autopsy. C shows the layered erythrocytes and no signs of organization.

heterogeneities according to chicken fat clot within the red-currant jelly clot. The chicken fat clots either presented in an adjacent (vertical) layered pattern (78.6 %) and only a few with horizontal layered portions (21.4 %).

The second often pattern was the presence of solely sediment (24.6 %), followed by the presence of a red currant jelly clot with sediment (21.1 %), then solely red currant jelly clot filling the entire pulmonary trunk and arteries (10.5 %) and finally a truncated red currant jelly clot along the pulmonary trunk and its bilateral pulmonary arteries (8.8 %).

The entire pulmonary trunk and the pulmonary arteries were filled with material in 24.5 % of all cruor cases (Fig. 5). The distribution according to the cruor pattern was as following: solely sediment 10.5 %, solely red-currant jelly clot 10.5% and red currant jelly clot with sediment 3.5 %.

In all cases where the entire pulmonary trunk and both arteries were filled with the red currant jelly clot a re-positioning of the cruor was not feasible. In one case of the group with red currant jelly clot combined with sediment re-positioning was also not feasible. All other cases from this group and the solely sediment group allowed re-positioning even if the entire pulmonary trunk and both arteries were filled with the material.

Motion artifacts on PMMR (sedimentation)

The re-positioning of the corpse led to postmortem motion artifacts in prone position in 23 cases (20.4 %) of the total case collective. The all cases the time ranged between the last sequence in supine position and the first sequence (after survey) from 7 to 114 min (mean 23.2 min, median 22 min). The cases with motion artifacts ranged from 7 to 25 min (mean 16.5 min, median 17 min) and the cases with no motion artifacts ranged from 13 to 114 min (mean 27.7 min, median 24 min).

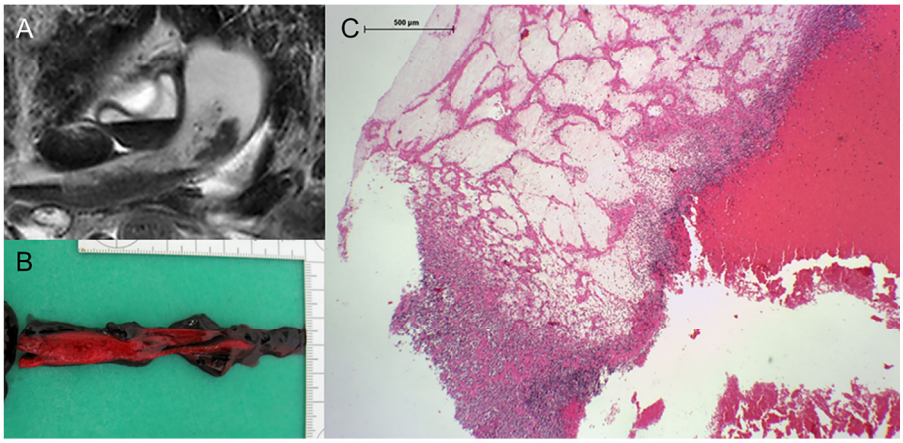

Fig. 6. (A) Shows PMMR in supine (left image) and prone (right image) position. Note the re-location of the cruor. The cruor consist of a portion of red currant jelly clot and chicken fat clot (B) on PMMR (A) and macroscopic assessment (B). Histology did confirm the findings of rather loose fibrin fiber meshwork and leukocytes in the chicken fat clot (left portion of the histology slide) and layered erythrocytes with no signs of organization (right portion of the histology slide).

Autopsy

The written reports and photographs showed in 45 % hyperacute PE (grade 1, n:9) (Fig. 2). Hyperacute to acute PE was described in 70 % (grade 1+2, n:14) and hyperacute to subacute in 80 % (grade 1-3, n:16) respectively (Fig. 1). Chronic PE (grade 4/5, n: 2) and mixed grading (grade 1+2+4, n:1; grade 2+4, n:1) was scarcely described (Fig. 4). Only macroscopic inspection yielded on case with grade 5 that was not confirmed in histology or PMMR.

Histology

Histology yielded 37.5 % with hyperacute PE (n:6), 68.8 % with hyperacute to acute PE (n:11) and 87.5 % with hyperacute to subacute PE (n:14) (Fig. 1). Isolated chronic grade 4 was seen in 6.3 % (n:1) and combined grade 1+4 also in 6.3 % (n:1) (Table 1).

Discussion

Comparison of PMMR, autopsy and histology

Histology is certainly still considered the gold standard for the determination of PE and its detectable grade of organization (age) [30]. However, the obtained specimens are cut in slices for microscopic assessment and the evaluated parts by microscope will usually only represent a small portion that was stained for analysis. Other portions with a different age grading of the PE might be missed (Fig. 1). Most pulmonary emboli are multiple-phased and therefore have different ages. Histological specimens are therefore an excerpt of the entire PE.

On PMMR on the other hand the investigator has the complete pulmonary trunk and both main pulmonary arteries for evaluation and based on the signal intensity differences a more precise evaluation is feasible, as all portions of the clot are visible in the major vessels. Segmental vessels are harder to assess, subsegmental arteries were deemed as not feasible to assess and therefore the evaluation was centered on the major vessels. However, this poses currently a limitation to the detection of PE on PMMR. Although, peripheral PE may also not be the cause of death which is the major inquiry for radiological detection in a forensic setting.

Autopsy allows for the assessment of the entire pulmonary trunk, main pulmonary arteries and peripheral vessels, if dissected accurately into the periphery of each lobe. The macroscopic assessment on the other hand is based on subjective estimation, experience and is not reproducible unlike postmortem image evaluation. Photographs may aid for a more objective evaluation but is also prone to bias.

PMMR revealed only 20 % with an isolated morphology grade, but 80 % with combined grades. Histology showed isolated grades in 56.2 % and combined grades in 43.8 %. Autopsy detected isolated grades in 60 % and combined grades in 40 % of the cases with PE. The differing results may be explicable by the above-mentioned reasons (Table 3).

However, the majority of cases presented with a combined morphology ranging from hyperacute to subacute PE, indicating that PE is an progressive process. A smaller percentage exhibited hyperacute PE as cause of death (Table 3). This outcome aligns with established literature, asserting that predominantly mixed thrombi, adherent to the vessel wall, appear as “white-gray” with a “red” tail. The section of the thrombus in contact with the bloodstream displays the characteristics of a mixed thrombus, whereas the portion freely floating within the bloodstream shows the characteristics of a red coagulation thrombus [30].

Motion artifacts on PMMR

Motion artifacts are unknown in postmortem imaging unlike clinical imaging. However, they do occur due to gravity and re-positioning of corpses or due to insect infestation. This study did prove in 1/5 of the cases (20.4 %) that re-positioning with a short time interval from supine to prone position led to sinking of the organs gravity-dependent with subsequent motion artifacts on PMMR. This is firstly described by this underlying study and should be taken into account when planning PMMR. After re-positioning at least 15 to 20 min should elapse before imaging is preceded if the position of the corpse was changed in a 180-degree manner and so motion artifacts should be avoided. Cases that did not present with motion artifacts but with a short interval between the re-positioning did all present with accompanying pathologies such as vast pleural effusion, sero-fibro thorax or massive pulmonary edema. The authors hypothesize that such pathologies may affect and minimize the occurrence of motion artifacts and would need further investigation for postmortem imaging.

Table 3
The percentage of cases (n=20) with PE in relation to its grading in histology, autopsy and PMMR.

Grade of PE	Histology (%)	Autopsy (%)	PMMR (%)
Hyperacute	37.5 %	45 %	5 %
Hyperacute-acute	68.8 %	70 %	35 %
Hyperacute-subacute	87.5 %	80 %	65 %
Chronic	6.3 %	10 %	10 %
Combined morphology	43.8 %	40 %	80 %

Discrimination between PE and postmortem clotting

Re-positioning the corpse from supine in prone position proved to be beneficial in order to discriminate PE from cruor due to the re-distribution of plasma and sediment and the delineation of the wall-adherence. The exception may be if PE is hyperacute and no reaction between the endothelium and thrombus has occurred, although the 10 % in this study showed only partial movement. Cruor did always re-locate in prone position, except in cases with an entirely filled pulmonary trunk and both main arteries (< 25 %) as there was no or only little space for movement. One case with a vast red currant jelly clot combined with sediment did also not relocate. The authors hypothesize that this occurred due to the vast extent of the red currant jelly clot. Based on this study PMMR imaging in prone after supine position should be performed if supine position does not deliver a clear diagnosis on PE or ruling out PE. A limitation to this study is certainly that prone position was not always performed, either to time issues or if diagnosis was already obtained by supine PMMR images. Additionally, a larger scale study with positive PE would be desirable. Another limitation poses the incomplete histology of 16 but 20 cases with PE.

Chicken fat clots occurrence is described to be related to the survival time (more than 1 day before death) [34]. This fact goes along with the investigated case collective (35 % of the cruor cases) and thereof the presence of a portion of the postmortem clot as chicken fat clot in 70 % to variable extents [5,34].

Postmortem imaging of PE in literature

There is scarce literature on the topic on PE imaged although there remains a high diagnostic insecurity in determining precisely, if the clot is PE or cruor [5,27,29,31,35–38]. Jackowski et al. (2012) was the first to describe the appearance of PE on 3T PMMR based on a study population of 8 cases [36]. This study found in all cases positive on PE homogenous material within the main pulmonary artery and / or pulmonary artery branches [36]. The signal intensity was described as intermediate signal [36]. The differential of cruor was determined as floating free near the boundary between serum and erythrocytes [36]. These results differ from those of the underlying study as it revealed that the signal intensities and morphology of PE is dependent on the age (grade) of the vitally embolized clot and that cruor has also distinct but multitude patterns on PMMR. The reason for the differing results on the same PMMR scanner may be explicable by the smaller case number imaged, potentially all presenting with only hyperacute isolated grading of PE on PMMR. The authors may have had an isolated case collective and therefore have drawn their conclusion towards describing PE on PMMR as homogenous with intermediate signal intensity as the present underlying study found different signal intensities and homogeneity according to differing organization and age of PE.

The approach chosen by Jackowski et al. (2012) in additionally imaging the lower legs in 3 cases and to assess for deep venous thrombosis is certainly beneficial [36]. However, the presence of deep vein thrombosis and its detection may support the final potential diagnosis of PE but not prove it nor rule it out. Ampanozi et al. (2016) combined the evaluation of the lower extremities and the pattern analysis of material within the pulmonary trunk and its main arteries on PMCT without contrast enhancement [35]. The authors evaluated the swelling of both legs by areal measurement but yielded no statistical difference in the PE and control group [35]. But PE cases did exhibit changes such as imbibition of the fatty tissue surrounding the deep veins of the lower extremities. The focal perivascular soft tissue edema was present in 67 % of the PE cases and was statistically significant compared to the controls [35]. The authors also described a distinct pattern of irregular shaped (hyper- to hypodense) content of the material of the pulmonary trunk and the main pulmonary arteries [35]. Both diagnostic clues (perivascular edema in the lower limbs and irregular shaped content in the pulmonary trunk and main branches) aids in the assessment of PE on unenhanced PMCT but leaves space for diagnostic uncertainty [35].

Mueller et al. (2014) described other supporting imaging clues on PMCT [38]. Based on this study an increased diameter (cut-off value 12.5 mm) of the inferior cava vein was suggestive for PE [38]. However, they also acknowledged that other causes of right heart failure that may also cause the distension of the inferior cava vein [38].

Other studies chose the approach of using PMCT-angiography (PMCTA) by applying contrast media via a cannula through the femoral vein, preferably by firstly injecting in the venous system in order to visualize the pulmonary trunk prior to the arterial system [29,31]. Burke et al. (2014) investigated 13 cases with suspected PE as preliminary study (7 positive on PE, 6 negative on PE) and claim that negative studies appeared to be the easiest to diagnose and those cases with massive PE would also appear to be within the diagnostic capabilities if PMCT is routinely used [29]. Segmental PE is described as being problematic and the authors recommended autopsy [29]. They also state that referral to radiologists with experience on forensic cases would lead to a more robust diagnosis [29]. Burke et al. approach the postmortem clotting by searching for continuity of smooth-edged filling defects, unbroken from the right ventricle through to the main pulmonary trunk and left and right main pulmonary artery [29]. Another criterion for cruor was being formed in and reflecting the shape of the pulmonary arteries [29]. This described diagnostic pattern was only seen in less than 10 % of the postmortem clotting patterns in the underlying PMMR study (truncated red currant jelly clot collective 8.8 %). Alves et al. (2014) present a case with limited chest compression and peripherally injected contrast media as being sufficient for PMCTA of the pulmonary arteries and diagnosed findings being suggestive for PE [27]. The same study group additionally proposed by Picheraeau et al. (2015) that extensive defects of the pulmonary trunk, right atrium and ventricle may rather suggest cruor than PE [37].

The continuity of cruor to the heart chambers was not investigated in this study specifically but the signal intensity and morphology within the heart chambers (especially the left ventricle) and major vessels (e.g. caval vein) were used as comparison for aiding in diagnosis, but not as reliable criterion. This may pose a limitation to the underlying PMMR study.

Ross et al. (2014) performed PMCTA with antegrade perfusion of the venous system via the femoral vein [31]. The authors state that in cases with a prolonged agonal phase, filling defects of the segmental or subsegmental pulmonary arteries are often seen but not necessarily related to PE [31]. Small postmortem clots may be pushed by the contrast medium injection into the pulmonary periphery [31]. On the other hand they state that vast filling defects in the pulmonary trunk and both main pulmonary arteries may be primarily indicative for massive central PE [31]. However, they also state that diagnosis of PE has do be finally confirmed or ruled out by histopathology, e.g. by image-guided biopsy [31].

However, all the currently published studies on PMCT with or without contrast media pose the same obstacle: PE is not reliable distinguishable from postmortem clotting – except histology is obtained. Although the total of diagnostic clues combined may lead to a highly reliable diagnosis which should be further investigated in future by unenhanced PMCT, as this method is most readily available in a forensic setting nowadays.

The authors are positive that the ongoing research on PMMR will smooth the way for routine examination by PMMR as this method is complementary to PMCT and PMCTA and would certainly yield together a similar reliability as autopsy for diagnosing PE. According to the data obtained in this study the diagnosis PE can certainly be made by using the PMMR. Nevertheless, histology will still be a valuable asset regardless if postmortem imaging or autopsy is performed.

Conclusion

The current study shows that PMMR is a highly sensitive tool on the

detection of PE. It also allows for the determination of the age and composition of the thrombus based on its morphology and signal intensity, especially in cases of chronic thrombi.

Disclose

Nothing to disclose.

Funding

None.

CRediT authorship contribution statement

P.M. Flach: Conceptualization, Investigation, Methodology, Project administration, Supervision, Validation, Visualization, Writing – original draft. **S. Franckenberg:** Validation, Writing – review & editing. **D. Gascho:** Conceptualization, Data curation, Project administration. **G. Ampanozi:** Conceptualization, Data curation, Project administration. **M.J. Thali:** Resources. **B. Fliss:** Conceptualization, Formal analysis, Investigation, Methodology, Validation, Visualization, Writing – original draft.

Declaration of Competing Interest

The authors declare that they have no known competing financial interests or personal relationships that could have appeared to influence the work reported in this paper.

References

[1] M. Baglivo, S. Winklhofer, G.M. Hatch, G. Ampanozi, M.J. Thali, T.D. Ruder, The rise of forensic and post-mortem radiology–Analysis of the literature between the year 2000 and 2011, J. Forensic Radiol. Imaging 1 (2013) 3–9, https://doi.org/10.1016/j.jofri.2012.10.003.

[2] M.J. Thali, K. Yen, W. Schweitzer, P. Vock, C. Boesch, C. Ozdoba, G. Schroth, M. Ith, M. Sonnenschein, T. Doernhoefer, E. Scheurer, T. Plattner, R. Dirnhofer, Virtopsy, a new imaging horizon in forensic pathology: virtual autopsy by postmortem multislice computed tomography (MSCT) and magnetic resonance imaging (MRI)–a feasibility study, J. Forensic Sci. 48 (2003) 386–403.

[3] M.J. Thali, B.G. Brogdon, M.D. Viner, Brogdon's Forensic Radiology, Second Edition, 2nd ed., CRC Press, Boca Raton, 2010.

[4] M.J. Thali, R. Dirnhofer, P. Vock, The Virtopsy Approach, CRC Press, Boca Raton, 2009. http://www.crcpress.com/product/isbn/9780849381782. accessed July 16, 2014.

[5] P.M. Flach, Imaging of the Pelvis, Musculoskeletal System, and Special Applications to CAD, CRC Press, 2016.

[6] G.N. Rutty, B. Morgan, C. O'Donnell, P.M. Leth, M. Thali, Forensic institutes across the world place CT or MRI scanners or both into their mortuaries, J. Trauma 65 (2008) 493–494, https://doi.org/10.1097/TA.0b013e31817de420.

[7] E.C. Burton, M. Mossa-Basha, To image or to autopsy? Ann. Intern. Med. 156 (2012) 158–159, https://doi.org/10.7326/0003-4819-156-2-201201170-00014.

[8] P.M. Flach, M.J. Thali, T. Germerott, Times have changed! Forensic radiology–a new challenge for radiology and forensic pathology, AJR Am. J. Roentgenol. 202 (2014) W325–W334, https://doi.org/10.2214/AJR.12.10283.

[9] T.D. Ruder, M.J. Thali, G.M. IIatch, Essentials of forensic post-mortem MR imaging in adults, Br. J. Radiol. 87 (2014), 20130567, https://doi.org/10.1259/bjr.20130567.

[10] T.D. Ruder, P. Stolzmann, Y.A. Thali, G.M. Hatch, S. Somaini, M. Bucher, H. Alkadhi, M.J. Thali, G. Ampanozi, Estimation of heart weight by post-mortem cardiac magnetic resonance imaging, J. Forensic Radiol. Imaging 1 (2013) 15–18, https://doi.org/10.1016/j.jofri.2012.11.001.

[11] T.D. Ruder, R. Bauer-Kreutz, G. Ampanozi, A.B. Rosskopf, T.M. Pilgrim, O. M. Weber, M.J. Thali, G.M. Hatch, Assessment of coronary artery disease by post-mortem cardiac MR, Eur. J. Radiol. 81 (2012) 2208–2214, https://doi.org/10.1016/j.ejrad.2011.06.042.

[12] C. Jackowski, M. Thali, E. Aghayev, K. Yen, M. Sonnenschein, K. Zwygart, R. Dirnhofer, P. Vock, Postmortem imaging of blood and its characteristics using MSCT and MRI, Int. J. Leg. Med. 120 (2006) 233–240, https://doi.org/10.1007/s00414-005-0023-4.

[13] A.C.G. Breeze, F.A. Jessop, P.A.K. Set, A.L. Whitehead, J.J. Cross, D.J. Lomas, G. A. Hackett, I. Joubert, C.C. Lees, Minimally-invasive fetal autopsy using magnetic resonance imaging and percutaneous organ biopsies: clinical value and comparison to conventional autopsy, Ultrasound Obstet. Gynecol. Off. J. Int. Soc. Ultrasound Obstet. Gynecol. 37 (2011) 317–323, https://doi.org/10.1002/uog.8844.

[14] J.A. Brookes, M.A. Hall-Craggs, V.R. Sams, W.R. Lees, Non-invasive perinatal necropsy by magnetic resonance imaging, Lancet 348 (1996) 1139–1141, https://doi.org/10.1016/S0140-6736(96)02287-8.

[15] S. Thayyil, N.J. Sebire, L.S. Chitty, A. Wade, W. Chong, O. Olsen, R.S. Gunny, A. C. Offiah, C.M. Owens, D.E. Saunders, R.J. Scott, R. Jones, W. Norman, S. Addison, A. Bainbridge, E.B. Cady, E.D. Vita, N.J. Robertson, A.M. Taylor, MARIAS collaborative group, Post-mortem MRI versus conventional autopsy in fetuses and children: a prospective validation study, Lancet 382 (2013) 223–233, https://doi.org/10.1016/S0140-6736(13)60134-8.

[16] S. Thayyil, N.J. Sebire, L.S. Chitty, A. Wade, O. Olsen, R.S. Gunny, A. Offiah, D. E. Saunders, C.M. Owens, W.K.K. Chong, N.J. Robertson, A.M. Taylor, Post mortem magnetic resonance imaging in the fetus, infant and child: a comparative study with conventional autopsy (MaRIAS Protocol), BMC Pediatr. 11 (2011) 120, https://doi.org/10.1186/1471-2431-11-120.

[17] E.H. Whitby, M.N. Paley, M. Cohen, P.D. Griffiths, Postmortem MR imaging of the fetus: an adjunct or a replacement for conventional autopsy? Semin. Fetal Neonatal Med. 10 (2005) 475–483, https://doi.org/10.1016/j.siny.2005.05.006.

[18] A. Christe, P. Flach, S. Ross, D. Spendlove, S. Bolliger, P. Vock, M.J. Thali, Clinical radiology and postmortem imaging (Virtopsy) are not the same: specific and unspecific postmortem signs, Leg. Med. 12 (2010) 215–222, https://doi.org/10.1016/j.legalmed.2010.05.005. Tokyo Jpn.

[19] K. Yen, K.O. Lövblad, E. Scheurer, C. Ozdoba, M.J. Thali, E. Aghayev, C. Jackowski, J. Anon, N. Frickey, K. Zwygart, J. Weis, R. Dirnhofer, Post-mortem forensic neuroimaging: correlation of MSCT and MRI findings with autopsy results, Forensic Sci. Int. 173 (2007) 21–35, https://doi.org/10.1016/j.forsciint.2007.01.027.

[20] J.G. Cha, D.H. Kim, D.H. Kim, S.H. Paik, J.S. Park, S.J. Park, H.K. Lee, H.S. Hong, D.L. Choi, K.M. Yang, N.E. Chung, B.W. Lee, J.S. Seo, Utility of postmortem autopsy via whole-body imaging: initial observations comparing MDCT and 3.0 T MRI findings with autopsy findings, Korean J. Radiol. Off. J. Korean Radiol. Soc. 11 (2010) 395–406, https://doi.org/10.3348/kjr.2010.11.4.395.

[21] L. Patriquin, A. Kassarjian, M. O'Brien, C. Andry, S. Eustace, Postmortem whole-body magnetic resonance imaging as an adjunct to autopsy: preliminary clinical experience, J. Magn. Reson. Imaging 13 (2001) 277–287.

[22] S. Ross, L. Ebner, P. Flach, R. Brodhage, S.A. Bolliger, A. Christe, M.J. Thali, Postmortem whole-body MRI in traumatic causes of death, AJR Am. J. Roentgenol. 199 (2012) 1186–1192, https://doi.org/10.2214/AJR.12.8767.

[23] T.D. Ruder, G.M. Hatch, L.C. Ebert, P.M. Flach, S. Ross, G. Ampanozi, M.J. Thali, Whole body postmortem magnetic resonance angiography: postmortem MR Angiography, J. Forensic Sci. 57 (2012) 778–782, https://doi.org/10.1111/j.1556-4029.2011.02037.x.

[24] A. Torbicki, A. Perrier, S. Konstantinides, G. Agnelli, N. Galiè, P. Pruszczyk, F. Bengel, A.J.B. Brady, D. Ferreira, U. Janssens, W. Klepetko, E. Mayer, M. Remy-Jardin, J.P. Bassand, A. Vahanian, J. Camm, R. De Caterina, V. Dean, K. Dickstein, G. Filippatos, C. Funck-Brentano, I. Hellemans, S.D. Kristensen, K. McGregor, U. Sechtem, S. Silber, M. Tendera, P. Widimsky, J.L. Zamorano, J.L. Zamorano, F. Andreotti, M. Ascherman, G. Athanassopoulos, J. De Sutter, D. Fitzmaurice, T. Forster, M. Heras, G. Jondeau, K. Kjeldsen, J. Knuuti, I. Lang, M. Lenzen, J. Lopez-Sendon, P. Nihoyannopoulos, L. Perez Isla, U. Schwehr, L. Torraca, J. L. Vachiery, Guidelines on the diagnosis and management of acute pulmonary embolism: the task force for the diagnosis and management of acute pulmonary embolism of the European Society of Cardiology (ESC), Eur. Heart J. 29 (2008) 2276–2315, https://doi.org/10.1093/eurheartj/ehn310.

[25] J. Bělohlávek, V. Dytrych, A. Linhart, Pulmonary embolism, part I: epidemiology, risk factors and risk stratification, pathophysiology, clinical presentation, diagnosis and nonthrombotic pulmonary embolism, Exp. Clin. Cardiol. 18 (2013) 129–138.

[26] C.S. Landefeld, M.M. Chren, A. Myers, R. Geller, S. Robbins, L. Goldman, Diagnostic yield of the autopsy in a university hospital and a community hospital, N. Engl. J. Med. 318 (1988) 1249–1254, https://doi.org/10.1056/NEJM198805123181906.

[27] M. Alves, N. Bigé, E. Maury, L. Arrivé, Pulmonary embolism diagnosed by contrast-enhanced virtopsy, Am. J. Respir. Crit. Care Med. 189 (2014) 358–359.

[28] D.Y. Gong, X.F. Liu, F.J. Huang, Clinical feature analysis of fatal pulmonary thromboembolism: experiences from 41 autopsy-confirmed cases, Eur. Rev. Med. Pharmacol. Sci. 17 (2013) 701–706.

[29] M.P. Burke, P. Bedford, Y. Baber, Can forensic pathologists diagnose pulmonary thromboembolism on postmortem computed tomography pulmonary angiography? Am. J. Forensic Med. Pathol. 35 (2014) 124–131, https://doi.org/10.1097/PAF.0000000000000086.

[30] R. Dettmeyer, Forensic Histopathology: Fundamentals and Perspectives, 1st ed., Springer, Heidelberg, 2011, 2011. Corr. 5th printing 2013.

[31] S.G. Ross, M.J. Thali, S. Bolliger, T. Germerott, T.D. Ruder, P.M. Flach, Sudden death after chest pain: feasibility of virtual autopsy with postmortem CT angiography and biopsy, Radiology 264 (2012) 250–259.

[32] P.M. Flach, D. Gascho, W. Schweitzer, T.D. Ruder, N. Berger, S.G. Ross, M.J. Thali, G. Ampanozi, Imaging in forensic radiology: an illustrated guide for postmortem computed tomography technique and protocols, Forensic Sci. Med. Pathol. (2014), https://doi.org/10.1007/s12024-014-9555-6.

[33] W.G. Bradley, MR appearance of hemorrhage in the brain, Radiology 189 (1993) 15–26, https://doi.org/10.1148/radiology.189.1.8372185.

[34] I. Uekita, I. Ijiri, Y. Nagasaki, R. Haba, Y. Funamoto, T. Matsunaga, M. Jamal, W. Wang, M. Kumihashi, K. Ameno, Medico-legal investigation of chicken fat clot in forensic cases: immunohistochemical and retrospective studies, Leg. Med. 10 (2008) 138–142, https://doi.org/10.1016/j.legalmed.2007.11.004.

[35] G. Ampanozi, U. Held, T.D. Ruder, S.G. Ross, W. Schweitzer, J. Fornaro, S. Franckenberg, M.J. Thali, P.M. Flach, Pulmonary thromboembolism on

unenhanced postmortem computed tomography: feasibility and findings, Leg. Med. 20 (2016) 68–74, https://doi.org/10.1016/j.legalmed.2016.04.005.
[36] C. Jackowski, S. Grabherr, N. Schwendener, Pulmonary thrombembolism as cause of death on unenhanced postmortem 3T MRI, Eur. Radiol. 23 (2013) 1266–1270, https://doi.org/10.1007/s00330-012-2728-3.
[37] C. Pichereau, E. Maury, L. Monnier-Cholley, S. Bourcier, G. Lejour, M. Alves, J. L. Baudel, H. Ait Oufella, B. Guidet, L. Arrivé, Post-mortem CT scan with contrast injection and chest compression to diagnose pulmonary embolism, Intensive Care Med. 41 (2015) 167–168, https://doi.org/10.1007/s00134-014-3520-4.
[38] S.L. Mueller, Y. Thali, G. Ampanozi, P.M. Flach, M.J. Thali, G.M. Hatch, T. D. Ruder, Distended diameter of the inferior vena cava is suggestive of pulmonary thromboembolism on unenhanced post-mortem CT, J. Forensic Radiol. Imaging 3 (2015) 38–42, https://doi.org/10.1016/j.jofri.2014.11.006.